J Biomol NMR (2009) 43:229–238
DOI 10.1007/s10858-009-9305-3

ARTICLE

Methyl-detected 'out-and-back' NMR experiments for simultaneous assignments of Alaβ and Ileγ2 methyl groups in large proteins

Devon Sheppard · Chenyun Guo · Vitali Tugarinov

Received: 17 December 2008 / Accepted: 18 February 2009 / Published online: 10 March 2009

Abstract A set of sensitive methyl-detected 'out-and-back' NMR experiments for simultaneous assignments of Alaβ and Ileγ2 methyl positions in large proteins is described. The developed methodology is applied to an 82-kDa enzyme Malate Synthase G. Complete alanine β and isoleucine γ2 ^{1}H–^{13}C methyl chemical shift assignments could be obtained from the set of new methyl-detected 'out-and-back' 3D experiments. The described methodology for methyl assignments should be applicable to protein molecules within approximately 100-kDa molecular weight range irrespective of the labeling strategy chosen to produce selectively protonated Alaβ and Ileγ2 $^{13}CH_3$ sites on a deuterated background.

Keywords Methyl assignments · Methyl-TROSY · Isotope labeling · Large proteins

Abbreviations

TROSY	Transverse relaxation optimized spectroscopy
MQ	Multiple-quantum
HMQC	Heteronuclear multiple quantum correlation spectroscopy
MSG	Malate synthase G
ILV	Isoleucine, leucine, valine
DTT	Dithiothreitol

D. Sheppard · C. Guo · V. Tugarinov (✉)
Department of Chemistry and Biochemistry, University of Maryland, College Park, Maryland 20742, USA
e-mail: vitali@umd.edu

Introduction

Selective $^{13}CH_3$ labeling of Ile(δ1), Leuδ and Valγ (ILV) positions in large proteins on a deuterated background (Goto et al. 1999; Tugarinov and Kay 2004) coupled with Methyl-TROSY techniques (Tugarinov et al. 2003; Ollerenshaw et al. 2003) have had a significant impact on NMR studies of structure and dynamics in high-molecular-weight protein systems over the past several years (Hamel and Dahlquist 2005; Sprangers and Kay 2007; Sprangers et al. 2007; Tugarinov et al. 2004; Velyvis et al. 2007). The success of the ILV labeling methodology and associated NMR techniques is to a large extent predicated upon the availability of sensitive NMR experiments for methyl resonance assignments. Sensitive methyl-detected 'out-and-back' NMR experiments for $^{1}H^{m}$–$^{13}C^{m}$ assignments of selectively protonated ILV methyl groups in deuterated large proteins have been developed earlier by Kay and coworkers (Tugarinov et al. 2004; Tugarinov and Kay 2003). These experiments are significantly more sensitive than their HN-directed counterparts and have been used to obtain practically complete assignments of ILV methyls in an 82-kDa enzyme Malate Synthase G, MSG (Tugarinov and Kay 2003). Modified versions of these experiments have been instrumental for assignments of ILV methyls in the 20S proteasome core particle (Sprangers and Kay 2007). Methyl-detected NMR experiments for assignments of ILV methyls benefit from the isotope labeling strategy that 'linearizes' ^{13}C spin-systems of Leu and Val side-chains via the use of appropriate α-ketoacid biosynthetic precursors that have only one of their methyl positions labeled with $^{13}CH_3$ while the other remains deuterated and $^{12}C(^{12}CD_3)$, whereas the ^{13}C spin-systems of Ile side-chains have been 'linearized' spectroscopically by application of decoupling pulses selective for $^{13}C^{\gamma 2}$ methyl

positions (Tugarinov and Kay 2003). Such a linearization of ^{13}C homonuclear spin-systems of (branched) ILV side-chains has been shown to substantially simplify NMR spectra and provide sensitivity gains (Tugarinov and Kay 2003).

Clearly, the availability of only three ILV probes presents serious limitations for structural and dynamics studies of large protein systems. In search of additional probes for NMR studies we have targeted methyl groups of alanines (Alaβ) and γ2 methyl positions of isoleucines (Ileγ2). Selective protonation of these methyl sites can represent an attractive extension of the ILV labeling methodology. For example, alanine is one of the most abundant amino acids found in proteins (McCaldon and Argos 1988), and is the most abundant residue in MSG (10.1% of the amino-acid content); alanines are frequently encountered both in protein hydrophobic cores and at molecular interfaces (Fernandez et al. 2003). Importantly, Alaβ methyls are located in close proximity to the backbone; likewise, Ileγ2 positions are closer to the backbone than Ileδ1 methyls. Proximity to the backbone imparts less structural 'degrees of freedom' to these sites making them valuable additions and/or alternatives to ILV labeling methodology.

In contrast to ILV methyls, selective protonation of Alaβ and Ileγ2 sites can not be achieved by addition of suitable biosynthetic precursors to D_2O-based bacterial media. Recently, an isotope labeling strategy has been introduced for selective labeling of Ala methyls on a deuterated background (Isaacson et al. 2007). The proposed strategy uses 'rich' deuterated medium to avoid the scrambling of the isotope labels. On the other hand, over-expression of proteins in D_2O-based minimal media using pyruvate as the principal carbon source is known to result in substantial protonation of Alaβ, Ileγ2, Leuδ and Valγ methyl sites (Gardner and Kay 1998; Gardner et al. 1997; Rosen et al. 1996). In order to simultaneously protonate and assign as many (inaccessible so far) methyl sites as possible, we have chosen to use [U–^{13}C]-pyruvate as the main carbon source in D_2O-based minimal medium for generation protonated Alaβ and Ileγ2 methyls in MSG.

As a first step in extending the selective labeling strategy for large proteins beyond ILV positions, sensitive methods for methyl resonance assignments have to be devised. Recently, we developed a 4D ^{1}H–^{13}C NMR experiment for unambiguous assignments of Alaβ methyl positions in pyruvate-derived MSG from a single dataset (Sheppard et al. 2009). Here, we describe a set of sensitive methyl-detected 'out-and-back' 3D ^{1}H–^{13}C NMR experiments for simultaneous assignments of Alaβ and Ileγ2 sites in large and complex protein structures with an emphasis on Ileγ2 methyl assignments. The 'linearization' of ^{13}C spin-systems of Ile side-chains is achieved through application of Ile $^{13}C^{\gamma 1}$-selective pulses. Incidentally, such pulses leave unperturbed the Ala $^{13}C^{\beta}$ positions of the vast majority of alanines in MSG. Resonance assignments of 44 Ileγ2 and 73 Alaβ positions in MSG have been obtained using the developed NMR pulse-schemes. The developed methodology is expected to be applicable for assignments of Alaβ and Ileγ2 sites *irrespective* of the labeling strategy chosen for (selective) protonation of these non-ILV methyl sites in high-molecular-weight proteins.

Materials and methods

NMR sample

E.coli BL21(DE3)pLysS cells have been transformed with the plasmid pet-28b encoding for the sequence of MSG (Howard et al. 2000; Tugarinov et al. 2002). The cells were initially grown in 50 ml H_2O-based M9 medium using 0.3% D-glucose as the carbon source (M9/H_2O/glucose, 0.3%). At $OD_{600} = 0.8$, the cells were collected by centrifugation and re-suspended into 200 ml D_2O-based M9 medium containing [U–^{13}C]-pyruvate as the main carbon source (M9/D_2O/pyruvate, 0.3%). [U–^{13}C]-pyruvate was obtained from Isotec/Sigma-Aldrich (Miamisburg, OH). The cells were subsequently diluted step-wise into (i) 600 ml, and then (ii) 1 l of the (M9/D_2O/pyruvate, 0.15%) medium. To minimize exchange between pyruvate protons and solvent deuterons, the cells were grown in the (M9/D_2O/pyruvate, 0.15%) medium until induction (Gardner et al. 1997; Rosen et al. 1996). Upon induction of protein over-expression with 1 mM IPTG at $OD_{600} = 0.3$, additional pyruvate was added to the total concentration of 0.3%. Although the final cell-density in the pyruvate-based growth was somewhat lower than is normally achieved in glucose-based media, the final protein yield was comparable to that obtained from (M9/D_2O/glucose, 0.3%). Over-expressed MSG was purified as described previously (Howard et al. 2000; Tugarinov et al. 2002). The 0.9 mM protein sample was dissolved in 99.9% D_2O, and contained 25 mM sodium phosphate (pH 7.1, uncorrected), 0.05% NaN_3, 5 mM DTT, 20 mM $MgCl_2$ and a cocktail of protease inhibitors.

NMR spectroscopy

All experiments were performed on a Bruker Avance III 600 MHz spectrometer equipped with a pulsed-field gradient triple-resonance room-temperature probe operating at 37 °C. 2D ^{1}H–^{13}C constant time (CT) HMQC experiments (Bax et al. 1983; Mueller 1979) were acquired with the constant time period adjusted to $1/^{1}J_{CC} = 28$ ms and (66, 512) complex points in the (^{13}C, ^{1}H) dimensions with corresponding acquisition times of (27.2, 64 ms) and net experimental time of 40 min (16 scans/fid; relaxation delay

of 1 s). The 3D ALA-HMCMCA/ILE(γ2)-HMCMCB experiment providing correlations of the form [$\Omega_{C\alpha}$, $\Omega_{C\beta}$, $\Omega_{H\beta}$]([$\Omega_{C\beta}$, $\Omega_{C\gamma 2}$, $\Omega_{H\gamma 2}$]) for Ala(Ile) residues was recorded with 24 scans/fid and (18, 28, 512) complex points in (t_1, t_2, t_3) corresponding to acquisition times of (6, 13.2, 64 ms). Relaxation delay of 1 s led to total acquisition time of 15 h. The 3D ALA/ILE(γ2)-HMCMCA experiment providing correlations of the form [$\Omega_{C\alpha}$, Ω_{Cm}, Ω_{Hm}], where 'm' denotes either Alaβ or Ileγ2 methyl group, was recorded with 48 scans/fid and (12, 24, 512) complex points in (t_1, t_2, t_3) corresponding to acquisition times of (4.5, 13.2, 64 ms). The total experimental time was 17 h (relaxation delay of 1 s). The 3D ALA-HMCM(CA)CO spectrum providing correlations of the form [Ω_{CO}, $\Omega_{C\beta}$, $\Omega_{H\beta}$] has been recorded with 32 scans/fid and (12, 28, 512) complex points in (t_1, t_2, t_3) corresponding to acquisition times of (10, 13.2, 64 ms). The relaxation delay of 1 s resulted in total acquisition time of 13 h. The ILE(γ2)-HMCM(CBCA)CO experiment providing correlations of the form [Ω_{CO}, $\Omega_{C\gamma 2}$, $\Omega_{H\gamma 2}$] has been acquired with 128 scans/fid and (10, 28, 512) complex points in (t_1, t_2, t_3) corresponding to acquisition times of (8.3, 13.2, 64 ms) resulting in total experimental time of 44 h. (relaxation delay of 1 s). All NMR data were processed using NMRPipe/NMRDraw suite of programs (Delaglio et al. 1995). NMR spectra were analyzed with the NMRView program (Johnson and Blevins 1994) and home-written tcl/tk scripts using the previously determined $^{13}C^{\alpha}$,$^{13}C^{\beta}$,^{13}CO chemical shift assignments of alanines and isoleucine residues in MSG (Tugarinov et al. 2002).

Results and discussion

Selective methyl protonation via the use of pyruvate as a carbon source

Figure 1 shows the methyl region of the ^{1}H–^{13}C CT-HMQC correlation map recorded on MSG obtained from the bacterial medium using [U–^{13}C]-pyruvate as the main source of carbon (see 'Materials and Methods'). The spectrum was 'filtered' for $^{13}CH_3$ (against $^{13}CHD_2$) isotopomers as described earlier by (Gardner and Kay 1998; Gardner et al. 1997). $^{13}CHD_2$ was the only other methyl isotopomer present in observable quantities in the spectra of [U–^{13}C]-pyruvate-derived MSG. However, the generation of a significant portion of (undetectable) $^{13}CD_3$ groups together with the methyls of $^{13}CHD_2$ and $^{13}CH_2D$ variety, lead to a relatively low percentage of $^{13}CH_3$ isotopomers of interest (Rosen et al. 1996). As has been estimated from comparisons of $^{13}CH_3$ peak intensities in selectively methyl-labeled [2-^{13}C]-pyruvate-derived and {U-[^{2}H,^{15}N]; Ileδ1-[$^{13}CH_3$]; Leu,Val-[$^{13}CH_3$/$^{12}CD_3$]}-labeled samples with the same protein content, maximum ~25% (~30%) of the total isotopomer content at Alaβ(Ileγ2) positions are $^{13}CH_3$-labeled in [U–^{13}C]-pyruvate-derived MSG. This represents a clear disadvantage of the pyruvate-based isotope labeling strategy. In agreement with several earlier reports (Gardner et al. 1997; Rosen et al. 1996), in addition to Alaβ and Ileγ2 methyls, the [U–^{13}C]-pyruvate-derived samples of MSG contained (partially) protonated Valγ and Leuδ methyl sites (Fig. 1), as well as C^{γ}(C^{β}) positions in Arg, Pro, Glx(Asx, Ser, Trp). As described earlier by (Rosen et al. 1996), $^{13}C^{\alpha}$ positions of Ala and $^{13}C^{\alpha}$/$^{13}C^{\beta}$ positions of Ile are completely deuterated in protein molecules obtained in D_2O-based minimal media with pyruvate as the sole carbon source.

Both Alaβ and Ileγ2 methyl chemical shifts tend to be ill-dispersed in proteins (Fig. 1). For example, 88% of Ala methyls in MSG are clustered between 1.0 and 1.7 ppm (17 and 21 ppm) in the ^{1}H(^{13}C) dimension (Sheppard et al. 2009). The Alaβ and Ileγ2 regions of the ^{1}H–^{13}C correlation map overlap with each other to some extent, while both regions overlap with the region of Valγ methyl resonances, the latter assigned previously from methyl-detected experiments applied to the {U–[^{2}H,^{15}N,^{13}C]; Ileδ1-[$^{13}CH_3$]; Leu,Val-[$^{13}CH_3$/$^{12}CD_3$]}-labeled MSG (Tugarinov and Kay 2003). We note that the ILV (Ileδ1-$^{13}CH_3$;

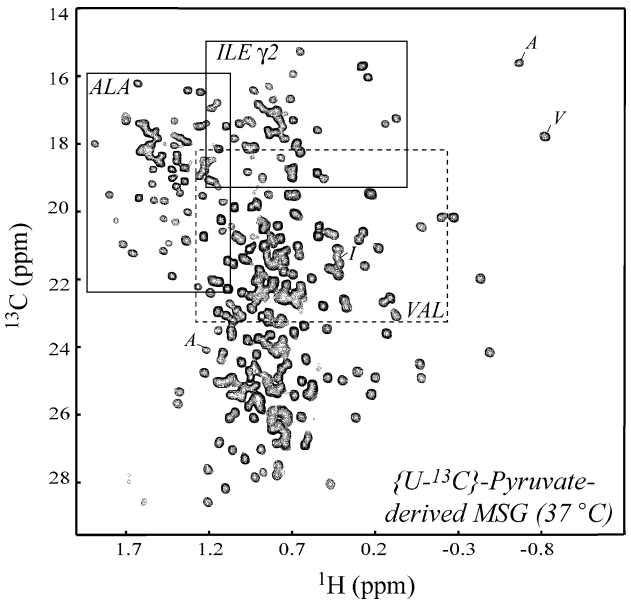

Fig. 1 The methyl region of the ^{1}H–^{13}C CT-HMQC correlation map recorded on a 0.9 mM [U–^{13}C]-pyruvate-derived sample of MSG (pH = 7.1; 37 °C) and 'filtered' for $^{13}CH_3$ (against $^{13}CHD_2$) isotopomers (Gardner et al. 1997). Approximate regions of Alaβ and Ileγ2 methyls are enclosed in solid rectangles, whereas the region corresponding to Valγ methyls is enclosed in a dashed rectangle. Outlying peaks of Ala, Val and Ile methyls are labeled with 'A,' 'V' and 'I,' respectively

Leu,Val-$^{13}CH_3/^{12}CD_3$) labeling strategy on a uniformly ^{13}C-labeled deuterated background (Tugarinov and Kay 2003) remains to be the method of choice for assignments of Valγ and Leuδ methyl positions in large proteins. Therefore, no attempt has been undertaken to develop NMR experiments for assignments of these positions in the [U–^{13}C]-pyruvate-derived MSG. Interestingly, since Val and Leu side chains in pyruvate-derived proteins are likely to be at least partially protonated at both methyl positions, the measured methyl ^{1}H–^{13}C MQ free-precession R_2 relaxation rates, sensitive to proximity of protons external to the methyl group of interest (Tugarinov and Kay 2004), prove to be on average 1.6-fold lower for Alaβ $^{13}CH_3$ sites than the MQ R_2 rates of Valγ and Leuδ methyls (25 ± 3.9

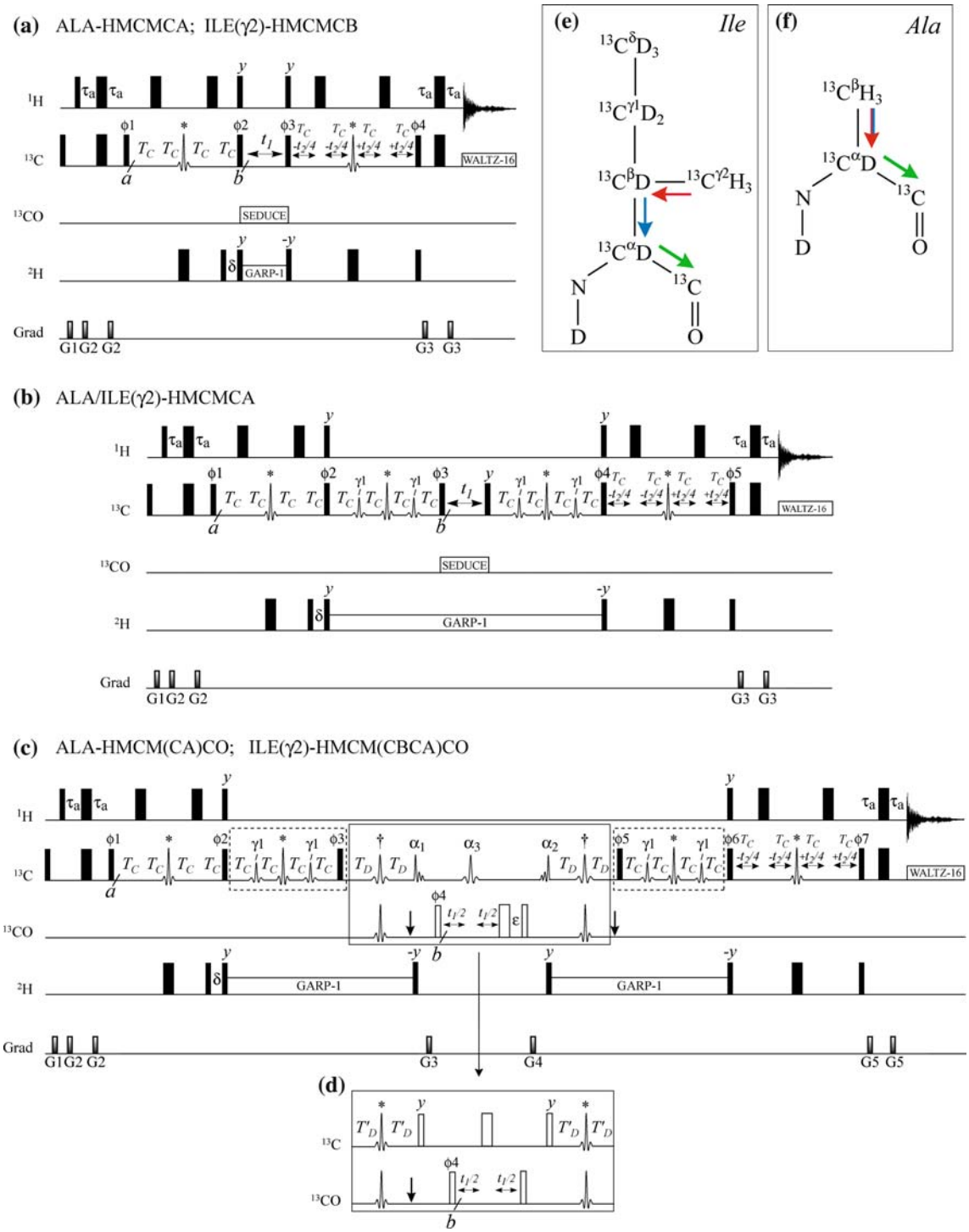

◀**Fig. 2** Methyl-detected 'out-and-back' pulse-schemes for simultaneous assignments of Alaβ and Ileγ2 methyl groups in large proteins. All narrow (wide) rectangular pulses are applied with the flip angles of 90° (180°). All pulses (including shaped pulses) are applied along the x-axis unless indicated otherwise. The $^{1}H(^{2}H)$ carrier is positioned at 4.7(2.5) ppm. All pulses shown with black rectangles are applied with the highest possible power. ^{13}C WALTZ-16 decoupling (Shaka et al. 1983) during acquisition is achieved using a 2.5 kHz field, while ^{2}H GARP-1 decoupling (Shaka et al. 1985) uses a 1.0 kHz field. SEDUCE ^{13}CO decoupling (McCoy and Mueller 1992) is implemented with 300 μ seduce-shaped pulses, with 137 ppm cosine-modulation of the waveform. The ^{13}C shaped pulses marked with asterisks are high-power 400 µs (600 MHz) RE-BURP pulses (Geen and Freeman 1991) applied on-resonance. It is important to adjust the phases of these RE-BURP pulses to maximize sensitivity. This can be accomplished by variation of the phase of each RE-BURP pulse separately around 0° (phase x) and choosing the value corresponding to maximum signal-to-noise in the spectrum. The ^{13}C pulses marked with 'γ1' are 4.0 ms (600 MHz) RE-BURP pulses selective for Ile $^{13}C^{\gamma 1}$ positions and are applied at 27 ppm by phase-modulation of the carrier (Boyd and Soffe 1989; Patt 1992). Delays are: $\tau_a = 2.0$ ms; $T_C = 3.5$ ms; $\delta = 1.4$ ms. **a** 3D ALA-HMCMCA/ILE(γ2)-HMCMCB pulse scheme. The ^{13}C carrier is placed at 18 ppm (the center of the Alaβ/Ileγ2 methyl region), switched to 40 ppm before the ^{13}C pulse with phase ϕ1 and returned back to 18 ppm after the pulse with phase ϕ4. The phase-cycle is: $\phi1 = x, -x$; $\phi2 = 2(y), 2(-y)$; $\phi3 = 4(y), 4(-y)$; $\phi4 = x$; rec. $= x, -x$. Quadrature in F_1 is achieved in the States-TPPI manner by incrementation of ϕ1 and ϕ2 by 90°, with 180° added to ϕ1 and the receiver for each successive complex t_1 point (Marion et al. 1989). Quadrature in F_2 is achieved via States-TPPI (Marion et al. 1989) of ϕ4. Durations and strengths of the pulsed-field gradients in units of (ms; G/cm) are: G1 = (1.0;10), G2 = (0.3;8), G3 = (0.4;10). **b** 3D ALA-HMCMCA/ILE(γ2)-HMCMCA pulse-scheme. The ^{13}C carrier is placed at 18 ppm, switched to 40 ppm before the ^{13}C pulse with phase ϕ1 and returned back to 18 ppm after the pulse with phase ϕ5. The phase-cycle is: $\phi1 = x, -x$; $\phi2 = 2(y), 2(-y)$; $\phi3 = y$; $\phi4 = 4(y), 4(-y)$; $\phi5 = x$; rec. $= x, -x$. Quadrature in F_1 is achieved in the States-TPPI manner by incrementation of ϕ1, ϕ2 and ϕ3 by 90°, with 180° added to ϕ1 and the receiver for each successive complex t_1 point. Quadrature in F_2 is achieved by States-TPPI of ϕ5. Durations and strengths of the pulsed-field gradients in units of (ms;G/cm) are: G1 = (1.0;10), G2 = (0.3;8), G3 = (0.4;10). **c–d** 3D ALA-HMCM(CA)CO/ILE(γ2)-HMCM(CBCA)CO pulse-schemes. Omission of the pulse scheme element enclosed in the dashed rectangle in (**c**) leads to the experiment for alanines, ALA-HMCM(CA)CO, while the complete scheme is employed for Ile residues, ILE(γ2)-HMCM(CBCA)CO. The pulse element shown in (**d**) corresponds to the 'non-selective' version of the experiment (see text). The ^{13}C carrier is placed at 18 ppm, switched to 40 ppm before the ^{13}C pulse with phase ϕ1, to 177 ppm before the pulse with phase ϕ4 and then returned to 40 ppm after the second ^{13}CO (open) 90° pulse following the t_1 period, and back to 18 ppm after the pulse with phase ϕ7. The ^{13}CO shaped pulses are 400 µs (600 MHz) RE-BURP pulses applied at 177 ppm by phase modulation of the carrier (Boyd and Soffe 1989; Patt 1992). The 90°(180°) ^{13}C pulses shown with open rectangles are applied with a field strength of $\Delta/\sqrt{15}(\Delta/\sqrt{3})$, where Δ is the difference (in Hz) between the $^{13}C^{\alpha}$ and ^{13}CO chemical shifts (Kay et al. 1990), and centered at 53(61) ppm for Ala(Ile) by phase modulation of the carrier. Vertical arrows at the end of $2T_D$ periods indicate the position of the ^{13}CO Bloch-Siegert compensation pulses (Kay et al. 1990). ^{13}C shaped pulses marked with daggers are 1.5 ms RE-BURP pulses applied at 53(61) ppm for Ala(Ile) via phase modulation of the carrier. $^{13}C^{\alpha}$-selective excitation pulses marked with 'α_1' and 'α_2' are 1.5 ms time-reversed-SNEEZE and SNEEZE pulses, respectively (Nuzillard and Freeman 1994) applied at 53(61) ppm for Ala(Ile) by phase modulation of the carrier. The pulse marked with 'α_3' is a 1.5 ms inversion pulse of a RE-BURP variety applied at 53(61) ppm for Ala(Ile). Delays $T_D(T_D')$ are adjusted to 4.50(4.75) ms; $\varepsilon = 1.5$ ms (equal to the length of the α_3 pulse). The phase-cycle is: $\phi1 = x, -x$; $\phi2 = \phi3 = 2(y), 2(-y)$; $\phi4 = 2(x), 2(-x)$; $\phi5 = \phi6 = 4(y), 4(-y)$; $\phi7 = x$; rec. $= x, -x, -x, x$. Quadrature in $F_1(F_2)$ is achieved by States-TPPI of $\phi4(\phi7)$. Durations and strengths of the pulsed-field gradients in units of (ms;G/cm) are: G1 = (1.0;10), G2 = (0.3;8), G3 = (0.8;12), G4 = (1.2;16), G5 = (0.4;10). Shown at the right top of the figure are schematic diagrams of the magnetization transfer steps employed for **e** Ile and **f** Ala residues. The flow of magnetization between time points a and b of the ALA-HMCMCA/ILE(γ2)-HMCMCB, ALA-HMCMCA/ILE(γ2)-HMCMCA, and ALA-HMCM(CA)CO/ILE(γ2)-HMCM(CBCA)CO experiments are indicated with red, blue and green arrows, respectively

vs. 40 ± 10.5 s^{-1} on average quantified for 28 Alaβ and 94 Valγ/Leuδ peaks, respectively).

Methyl-detected 'out-and-back' pulse schemes for simultaneous assignments of Alaβ and Ileγ2 methyls in high-molecular-weight proteins

Figure 2 shows the pulse-schemes for 3D ALA-HMCMCA/ILE(γ2)-HMCMCB (Fig. 2a), 3D ALA/ILE(γ2)-HMCMCA (Fig. 2b), and 3D ALA-HMCM(CA)CO/ILE(γ2)-HMCM(CBCA)CO (Fig. 2c) experiments developed for simultaneous assignments of Alaβ and Ileγ2 methyl groups in large proteins. The pulse-schemes are based upon the methyl-detected 'out-and-back' methodology developed earlier for ILV assignments in {U-[^{2}H,^{15}N,^{13}C]; Ileδ1-[$^{13}CH_3$]; Leu,-Val-[$^{13}CH_3$/$^{12}CD_3$]}-labeled protein samples (Tugarinov and Kay 2003). The 3D ALA-HMCMCA/ILE(γ2)-HMCMCB scheme (Fig. 2a) provides intra-residual correlations of the form [$\Omega_{C\alpha}$, $\Omega_{C\beta}$, $\Omega_{H\beta}$]([$\Omega_{C\beta}$, $\Omega_{C\gamma2}$, $\Omega_{H\gamma2}$]) in Ala(Ile) residues. The flow of magnetization from point a to point b can be represented as,

$$2H_x^m C_y^{\gamma 2} \xrightarrow{4T_C, 90_y, 90_{\varphi_2}} 4H_z^m C_z^{\gamma 2} C_x^{\beta}(t_1) \quad (1)$$

for alanines and,

$$2H_x^m C_y^{\gamma 2} \xrightarrow{4T_C, 90_y, 90_{\varphi_2}} 4H_z^m C_z^{\gamma 2} C_x^{\beta}(t_1) \quad (2)$$

for isoleucines, where C_r^i and $H_r^m = H_r^1 + H_r^2 + H_r^3$ are product operators for carbon nucleus i and the three methyl proton nuclei, respectively, $r = x, y, z$, and we concentrate on the first step of the phase cycle only. The terms at the right hand side of Eqs. (1) and (2) evolve during the t_1 period, and the magnetization is transferred back to methyl carbons (evolving during t_2), and subsequently to methyl protons for detection by the reverse of the pathway.

The same analysis performed between points a and b of the 3D ALA/ILE(γ2)-HMCMCA scheme (Fig. 2b),

providing correlations of the form [$\Omega_{C\alpha}$, $\Omega_{C\beta}$, $\Omega_{H\beta}$]([$\Omega_{C\alpha}$, $\Omega_{C\gamma 2}$, $\Omega_{H\gamma 2}$]) in Ala(Ile) leads to,

$$2H_x^m C_y^\beta \xrightarrow{4T_C,90_y,90_{\varphi_2}} 4H_z^m C_z^\beta C_x^\alpha \xrightarrow{4T_C,90_{\varphi_3}} -2H_z^m C_y^\alpha(t_1) \qquad (3)$$

for alanines and,

$$2H_x^m C_y^{\gamma 2} \xrightarrow{4T_C,90_y,90_{\varphi_2}} 4H_z^m C_z^{\gamma 2} C_x^\beta \xrightarrow{4T_C,90_{\varphi_3}} -4H_z^m C_z^\beta C_x^\alpha(t_1) \qquad (4)$$

for isoleucines. In this experiment, the 'linearization' of the isoleucine ^{13}C spin-system is achieved via application of ^{13}C RE-BURP pulses (Geen and Freeman 1991) selective for Ile $^{13}C^{\gamma 1}$ positions (pulses marked with '$\gamma 1$' in Fig. 2b). Figure 3a shows a theoretical inversion profile of such a 180° RE-BURP pulse. The $^{13}C^{\gamma 2}$ and $^{13}C^{\beta}$ nuclei of isoleucine side-chains remain unperturbed by this pulse. Fortuitously, such pulses (if applied at the center of the $^{13}C^{\gamma 1}$ region, 27 ppm) will not cover the vast majority of Alaβ positions (Fig. 3a). In MSG, $^{13}C^{\beta}$ of only two Ala residues, A467 ($^1H^{\beta}$ = 1.25 ppm; $^{13}C^{\beta}$ = 22.2 ppm) and A502 ($^1H^{\beta}$ = 1.20 ppm; $^{13}C^{\beta}$ = 24.1 ppm), resonate downfield of 22 ppm (Sheppard et al. 2009). As a result, all Ala correlations, except A467 and A502, are observed in the spectra, although the correlations with $^{13}C^{\beta}$ shifts between 21 and 22 ppm (corresponding to the resonance offsets of 905 and 755 Hz, respectively, at 600 MHz proton frequency) may be somewhat attenuated. This does not compromise Alaβ assignments, however, because all Ala $^{13}C^{\alpha}$ shifts are available at full intensity from the ALA-HMCMCA experiment (Fig. 2a). Note that the cross-peaks of Ala and Ile will have opposite signs in the final spectrum making it straightforward to distinguish between Ala and Ile correlations in the cases when their methyl chemical shifts fall in the same region of the 2D $^1H^m$–$^{13}C^m$ correlation map. The experiment in Fig. 2b can be modified in a straightforward manner (by adjusting the second $4T_C$ period of the scheme to $0.25/^1J_{CC}$) to obtain correlations to *both* $^{13}C^{\alpha}$ and $^{13}C^{\beta}$ (as well as Ile $^{13}C^{\gamma 2}$) nuclei in a single dataset. However, such a modification would (i) make it difficult to accommodate 4 ms-long $^{13}C^{\gamma 1}$-selective pulses within each $2T_C$ period (Fig. 2b), and (ii) generate carbon multiple-quantum coherences of the type $8H_z^m C_x^{\gamma 2} C_y^\beta C_x^\alpha$ for isoleucines. These terms would lead to appearance of 4 triple-spin peaks in the spectra (Tugarinov and Kay 2003) and unnecessarily complicate analysis.

The pair of 3D HMCMCB and HMCMCA experiments (Fig. 2a–b) alone applied to [U–^{13}C]-pyruvate-derived protein samples prove inconclusive in some cases because (i) the degeneracy of a substantial number of $^{13}C^{\alpha}/^{13}C^{\beta}$ chemical shift pairs precludes unambiguous assignments, and (ii) (aliased) cross-peaks arising from valine $^{13}C^{\beta/\alpha}$ positions may obscure the regions of interest containing Ala/Ile correlations of interest. To resolve the arising ambiguities, it is important to confirm the assignments using 3D

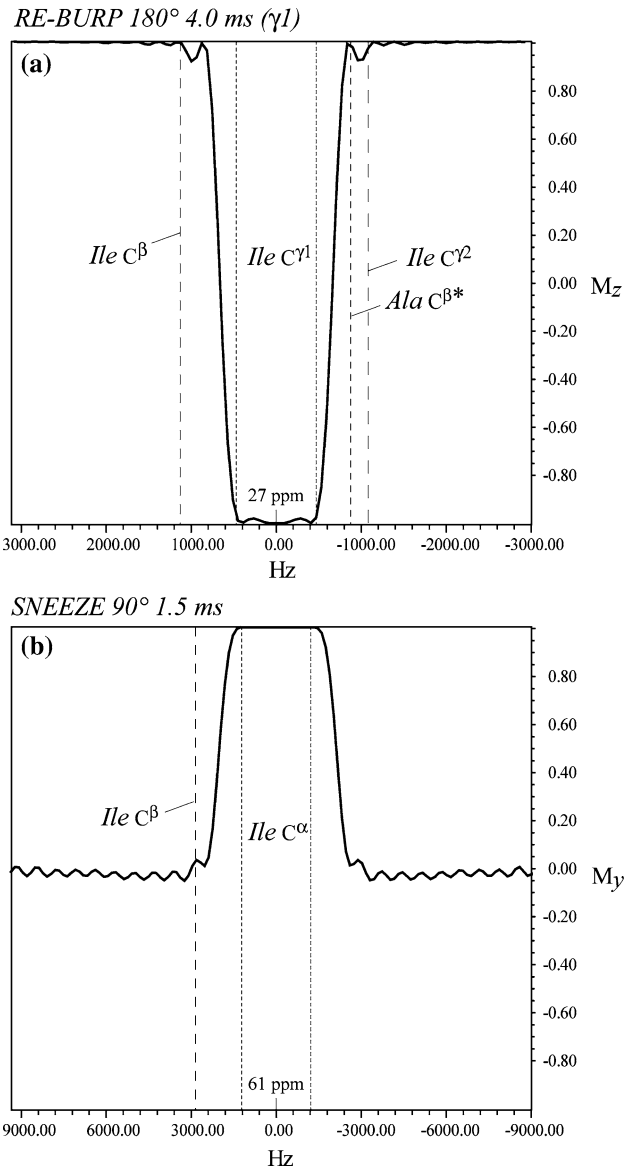

Fig. 3 Simulated inversion/excitation profiles of some selective ^{13}C pulses used in the pulse schemes of Fig. 2. **a** The inversion profile (M_z magnetization, *y*-axis, vs. resonance offset in Hz, *x*-axis) of a 4.0 ms RE-BURP 180° pulse (Geen and Freeman 1991) selective for $^{13}C^{\gamma 1}$ positions of isoleucines (pulse-schemes of Fig. 2b–d). **b** The excitation profile (M_y magnetization, *y*-axis, vs. resonance offset in Hz, *x*-axis) of a 1.5 ms SNEEZE 90° pulse (Nuzillard and Freeman 1994) selective for Ile $^{13}C^{\alpha}$ nuclei (marked 'α_2' in the pulse-scheme of Fig. 2c). Approximate limits of chemical shift ranges of the indicated ^{13}C nuclei at 600 MHz spectrometer ^{1}H frequency are shown with dashed vertical lines. The asterisk in **a** indicates that the majority of Ala $^{13}C^{\beta}$ resonances lie within the specified limit with the exception of A467 ($^1H^{\beta}$ = 1.25 ppm; $^{13}C^{\beta}$ = 22.2 ppm) and A502 ($^1H^{\beta}$ = 1.20 ppm; $^{13}C^{\beta}$ = 24.1 ppm)

ALA-HMCM(CA)CO/ILE(γ2)-HMCM(CBCA)CO experiments (Fig. 2c, d) that provide intra-residual correlations of the form [Ω_{CO}, $\Omega_{C\beta}$, $\Omega_{H\beta}$]([Ω_{CO}, $\Omega_{C\gamma 2}$, $\Omega_{H\gamma 2}$]) in Ala(Ile) residues. These experiments have been implemented in two versions. One version (denoted 'α-selective' in what follows)

employs $^{13}C^{\alpha}$-selective pulses in the element enclosed in a solid rectangle in Fig. 2c, and leads to the magnetization flow between points *a* and *b* (Fig. 2c),

$$2H_x^m C_y^{\beta} \xrightarrow{4T_C,90_y,90_{\varphi 2}} 4H_z^m C_z^{\beta} C_x^{\alpha} \xrightarrow{2T_D,\alpha_1,90_{\varphi 4}} -8H_z^m C_z^{\beta} C_z^{\alpha} C'_y(t_1) \quad (5)$$

for alanines (the scheme with the element enclosed in a dashed rectangle in Fig. 2c omitted) and,

$$2H_x^m C_y^{\gamma 2} \xrightarrow{4T_C,90_y,90_{\varphi 2}} 4H_z^m C_z^{\gamma 2} C_x^{\beta} \xrightarrow{4T_C,90_{\varphi 3}} -4H_z^m C_z^{\beta} C_x^{\alpha} \xrightarrow{2T_D,\alpha_1,90_{\varphi 4}} 8H_z^m C_z^{\beta} C_z^{\alpha} C'_y(t_1) \quad (6)$$

for isoleucines (with the 'dashed' element included in Fig. 2c). Another version of this experiment uses the pulse-scheme element employed previously in the 3D HMCM(CBCA)CO experiments for ILV assignments in {U-[^{2}H,^{15}N,^{13}C]; Ileδ1-[$^{13}CH_3$]; Leu,Val-[$^{13}CH_3$/$^{12}CD_3$]}-MSG (Tugarinov and Kay 2003) and shown in Fig. 2d. The magnetization flow between points *a* and *b* is then represented by (Fig. 2d),

$$2H_x^m C_y^{\beta} \xrightarrow{4T_C,90_y,90_{\varphi 2}} 4H_z^m C_z^{\beta} C_x^{\alpha} \xrightarrow{2T'_D,90_y,90_{\varphi 4}} 4H_z^m C_z^{\alpha} C'_y(t_1) \quad (7)$$

$$2H_x^m C_y^{\gamma 2} \xrightarrow{4T_C,90_y,90_{\varphi 2}} 4H_z^m C_z^{\gamma 2} C_x^{\beta} \xrightarrow{4T_C,90_{\varphi 3}} -4H_z^m C_z^{\beta} C_x^{\alpha} \xrightarrow{2T'_D,90_y,90_{\varphi 4}} -4H_z^m C_z^{\alpha} C'_y(t_1) \quad (8)$$

for Ala and Ile residues, respectively (only the terms that lead to observable magnetization in the end of the pulse-scheme are retained). Here, the carbonyl magnetization evolving during the t_1 period is in-phase with respect to $^{13}C^{\beta}$ spins.

Figure 3b shows the excitation profile of the $^{13}C^{\alpha}$-selective shaped pulses of the SNEEZE variety (Nuzillard and Freeman 1994), marked with '$\alpha_{1/2}$' in Fig. 2c, used to selectively excite $^{13}C^{\alpha}$ resonances of Ile residues. The 'α-selective' version of the experiment is expected to provide sensitivity gains as it modifies the transfer function during the $2T_D$ delay of the experiment from $\{\sin(2\pi\cdot{}^1J_{C\alpha C\beta}T_D')\ \sin(2\pi\cdot{}^1J_{C\alpha CO}T_D')\}^2 = 0.74$ (for $2T_D = 9.5$ ms used in the 'non-selective' experiment, Fig. 2d) to $\{\sin(2\pi\cdot{}^1J_{C\alpha CO}T_D)\}^2 = 1$ (for $2T_D = 9.0$ ms optimal for the 'α-selective' experiment, Fig. 2c). In practice, however, the 'α-selective' experiment proves to be even less sensitive than its 'non-selective' counterpart due to: (i) fast carbonyl relaxation (estimated $R_2^{CO} \sim 70\ s^{-1}$ for MSG in D_2O at 37°C; 600 MHz) during long selective pulses applied in the course of the t_1 period, and (ii) the length and possible imperfections of $^{13}C^{\alpha}$-selective pulses. The 'α-selective' approach of Fig. 2c has been tested for valines of MSG in comparison with the 3D VAL-HMCM(CA)CO experiment (Tugarinov and Kay 2003), both recorded on the {U-[^{2}H,^{15}N,^{13}C]; Ileδ1-[$^{13}CH_3$]; Leu,Val-[$^{13}CH_3$/$^{12}CD_3$]}-labeled MSG. The 'α-selective' VAL-HMCM(CA)CO experiment proved to be on average 15% less sensitive than its previously published (non-selective) counterpart. Sensitivity issues notwithstanding, we prefer to use the 'non-selective' version of the experiment for alanines (the 'dashed' element in Fig. 2c omitted), while the 'α-selective' version is recommended for isoleucines (the 'dashed' element in Fig. 2c included) as the latter provides spectra devoid of alanine correlations. In particular, the product operator analysis of the 'non-selective' version (Fig. 2d, with the 'dashed' element included) shows that the magnetization flow of the experiment would lead to generation of (significantly attenuated) coherences of the type $4H_z^m C_z^{\alpha} C'_y(t_1)$ in Ala residues. These terms would evolve with Ala ^{13}CO frequencies during the t_1 evolution period and appear in the 3D dataset together with correlations belonging to isoleucines. Although correlations of the form [Ω_{CO}, Ω_{Cm}, Ω_{Hm}] can be obtained in this manner for both Ala and Ile residues from a single experiment, such a magnetization transfer is far from being optimal for alanines. Therefore, we prefer to use separate experiments to obtain methyl-CO correlations for Ala and Ile residues.

The flow of magnetization from time-point *a* to time-point *b* in the experiments of Fig. 2 for Ile(Ala) sidechains is schematically illustrated in Fig. 2e, f). Importantly, all the pulse-schemes utilize the Methyl-TROSY principle (Tugarinov et al. 2003) where possible by keeping methyl magnetization ($^1H^{\beta}$–$^{13}C^{\beta}$/$^1H^{\gamma 2}$–$^{13}C^{\gamma 2}$) in a multiple-quantum state as long as it resides on carbons of methyl groups, i.e., before the $^{13}C\phi_2$/H_y pair of pulses and after the $^{13}C\phi_3$/H_y,$^{13}C\phi_4$/H_y($^{13}C\phi_6$/H_y) pairs of pulses in experiments of Fig. 2a, b (Fig. 2c). In order to eliminate the $^{13}CHD_2$ isotopomer signals from the spectra, the 180° ^{2}H pulses in the middle of $4T_C$ and t_2 periods ensure the evolution of $^1J_{C-D}$ couplings; subsequent application of ^{2}H 90° pulses at time-points approximately equal to $0.25/^1J_{C-D}$ eliminates most of the deuterium-containing magnetization terms in $^{13}CHD_2$ groups. No signals originating from $^{13}CHD_2$ isotopomers have been observed in any of the 3D datasets. As described earlier by Kay and co-workers (Gardner and Kay 1998; Gardner et al. 1997), it is not possible to eliminate all the lines of the $^{13}CD_2$ pentet simultaneously. Therefore, the delay chosen for $^1J_{C-D}$ evolution ($\sim 0.25/^1J_{C-D}$) is a compromise value that ensures acceptable suppression of $^{13}CHD_2$ isotopomers in practice. The choice of an exact value for this delay is of no consequence for the quality of $^{13}CHD_2$ suppression. To avoid complication of the t_2 evolution period, the second such ^{2}H 90° pulse is applied after the whole period of $4T_C$ (without an offset by delay δ, Fig. 2).

^{1}H–^{13}C resonance assignments of Alaβ and Ileγ2 methyls in MSG

In the case of alanines, all ^{13}C chemical shifts of the deuterated form of MSG are known from the previous NMR studies (Tugarinov et al. 2002), and the ^{1}H–^{13}C

assignment problem is seemingly reduced to identifying the correct $^{1}H^{\beta}$–$^{13}C^{\beta}$ connectivities in a 2D ^{1}H–^{13}C correlation map according to the known $^{13}C^{\beta}$ shifts (Sheppard et al. 2009). However, even this task can not be achieved without additional experiments due to severe degeneracy of many Ala $^{13}C^{\beta}$ chemical shifts (Fig. 1). The assignment problem is compounded by that $^{13}C^{\beta}$ chemical shifts in Ala $^{13}CH_3$ groups differ from those of $^{13}CD_3$ methyls by three times the value of one-bond deuterium isotope shift ($3[^{1}\Delta_{D \rightarrow H}] \approx 0.9$ ppm) (Gardner and Kay 1998; Venters et al. 1996) that is uniform only to within ±0.1 ppm (Sheppard et al. 2009). Therefore, protonated $^{13}C^{\beta}$ shifts in alanines of MSG are known only approximately. In contrast, alanine $^{13}C^{\alpha}$ shifts tend to be very close to the previously assigned values due to the compensatory effect of three times positive two-bond deuterium isotope shift, $3[^{2}\Delta_{D \rightarrow H}]$, that derives from the (protonated) methyl group, and one negative shift, $^{2}\Delta_{NH \rightarrow ND}$, derived from the amide proton substituted for a deuteron in the present study (Fig. 2f). In isoleucines, the $^{13}C^{\beta}$, $^{13}C^{\alpha}$ and ^{13}CO chemical shifts are available from the previous studies of the fully deuterated form of MSG (Tugarinov et al. 2002), with $^{13}C^{\beta}$ chemical shifts different from those in the 'out-and-back' data described here by the value of three times the two-bond deuterium isotope shift ($3[^{2}\Delta_{D \rightarrow H}] \approx 0.3$ ppm) due to protonation of the $\gamma 2$ methyl position (Fig. 2e). In either alanine or isoleucine case, the unambiguous methyl ^{1}H–^{13}C assignments are easily obtained by matching the ($^{13}C^{\beta}$), $^{13}C^{\alpha}$ and ^{13}CO chemical shifts from the set of 'out-and-back' experiments in Fig. 2 to those available from the previous studies after the isotope-shift corrections are taken into account as described above.

Figure 4 shows selected 2D $F_1(^{13}C^{\alpha}/^{13}C^{\beta}/^{13}CO)/F_3(^{1}H_m)$ slices of the 3D ALA-HMCMCA/ILE($\gamma 2$)-HMCMCB (Fig. 4a, b), 3D ALA/ILE($\gamma 2$)-HMCMCA (Fig. 4c, d), and 3D ALA-HMCM(CA)CO/ILE($\gamma 2$)-HMCM(CBCA)CO (Fig. 4e, f) experiments recorded on the [U–^{13}C]-pyruvate-derived MSG drawn at the F_2 chemical shift of Ala $^{13}C^{\beta} = 19.7$ ppm (Fig. 4, top row) and Ile $^{13}C^{\gamma 2} = 18.0$ ppm (Fig. 4, bottom row). Complete ^{1}H–^{13}C assignments of Alaβ and Ile$\gamma 2$ methyls in [U–^{13}C]-pyruvate-derived MSG have been obtained using the set of

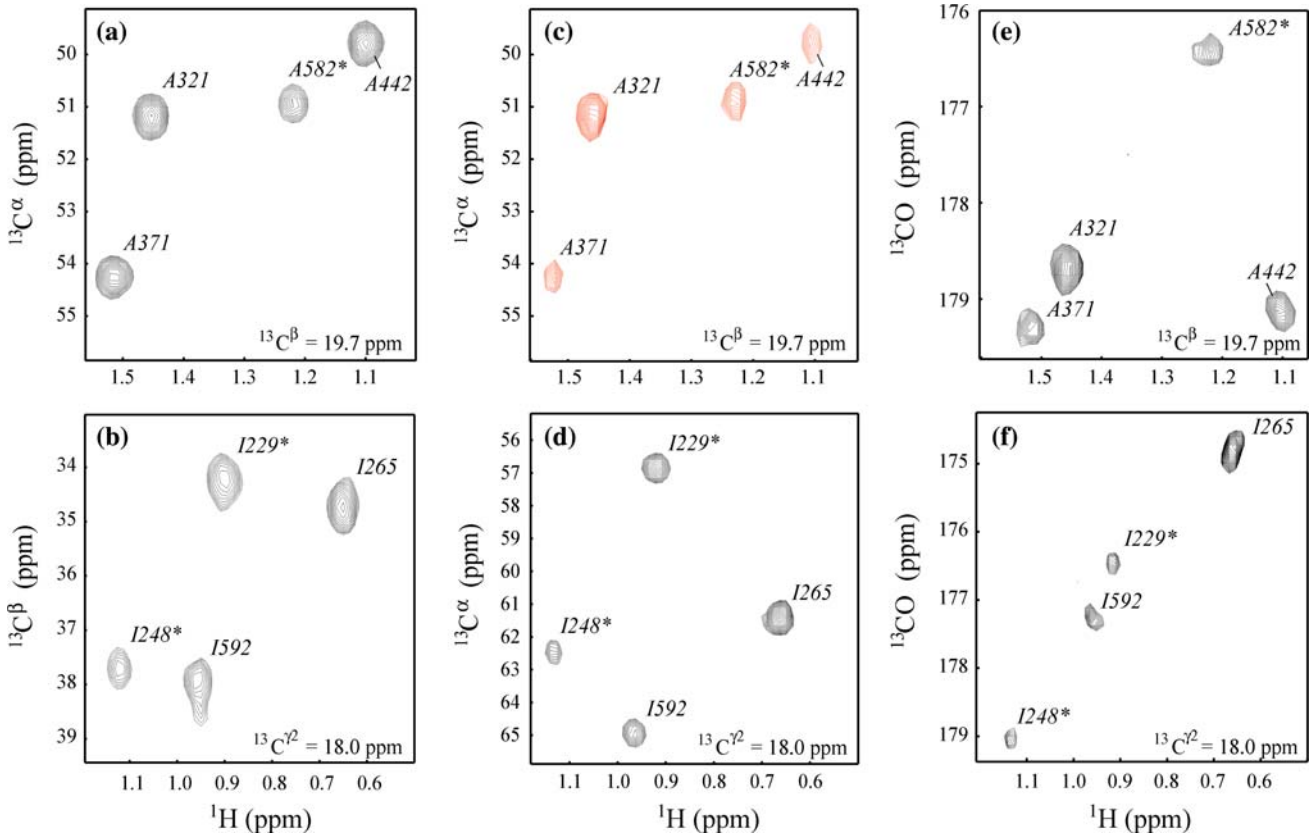

Fig. 4 Selected 2D F_1/F_3 slices from **a** ALA-HMCMCA, **b** ILE($\gamma 2$)-HMCMCB, **c** ALA-HMCMCA, **d** ILE($\gamma 2$)-HMCMCA, **e** ALA-HMCM(CA)CO, **f** ILE($\gamma 2$)-HMCM(CBCA)CO 3D experiments recorded on the [U–^{13}C]-pyruvate-derived MSG, drawn at the F_2 chemical shifts of Ala $^{13}C^{\beta} = 19.7$ ppm (*top row*) and Ile $^{13}C^{\gamma 2} = 18.0$ ppm (*bottom row*). The cross-peaks are labeled with residue numbers. Negative peaks are shown with red contours in (**c**). The maxima of the peaks marked with asterisks are located out of the planes shown in the figure

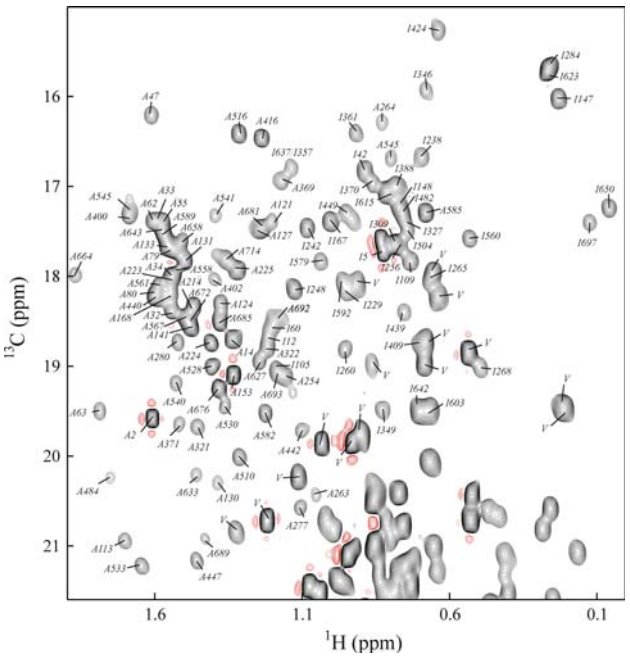

Fig. 5 The alanine $^{1}H^{\beta}$–$^{13}C^{\beta}$ and isoleucine $^{1}H^{\gamma 2}$–$^{13}C^{\gamma 2}$ region of a 2D methyl ^{1}H–^{13}C CT-HMQC spectrum shown in Fig. 1. Chemical shift assignments of Alaβ and Ileγ2 methyls are indicated with residue numbers. The peaks belonging to Val methyl signals assigned previously (Tugarinov and Kay 2003) are marked with 'V.' The I309 peak marked with an asterisk corresponds to a second conformation of MSG with an iso-aspartyl linkage between residues Asn305 and Gly306 (Tugarinov et al. 2002)

experiments in Fig. 2. The Alaβ-Ileγ2 region of a 2D methyl ^{1}H–^{13}C correlation map of Fig. 1 is 'zoomed' in Fig. 5 with Alaβ and Ileγ2 assignments marked with residue numbers. The Alaβ chemical shift assignments are in full agreement with those obtained in MSG using a single 4D ALA-HMCMCACO experiment developed by us earlier for unambiguous assignments of Alaβ positions exclusively (Sheppard et al. 2009).

The methyl assignment strategy based upon matching carbon chemical shifts from the set of 'out-and-back' experiments to those available from the previous studies is evidently predicated upon the availability of backbone and $^{13}C^{\beta}$ resonance assignments. Thus, the only remaining ambiguities in Ala and Ile methyl assignments are associated with residues for which no prior ^{13}C chemical shifts are available. For example, the assignments for I357 and I637 γ2 methyls are inter-changeable as chemical shifts for $^{13}C^{\beta}$, $^{13}C^{\alpha}$, and ^{13}CO nuclei are not known for these residues from earlier studies (Tugarinov et al. 2002). It is worth noting the possibility of alternative approaches to Alaβ and Ileγ2 methyl assignments in large proteins. For example, when ^{15}N–^{1}H amide assignments and the protein structure are known, Alaβ and Ileγ2 methyls can be assigned from HN-methyl NOEs which can be obtained using the simultaneous methyl-amide TROSY-based experiments (Guo and Tugarinov 2009). The assignment strategy based on NOEs has been demonstrated earlier on protonated protein samples by Yang and co-workers (Xu et al. 2005, 2006). It is, however, important to keep in mind that a certain degree of ambiguity, inevitably present in the NOE-based assignment approach, is avoided when assignments are based on (earlier established) ^{13}C chemical shifts.

In summary, we have presented a set of new methyl-detected 'out-and-back' NMR experiments for simultaneous assignments of Alaβ and Ileγ2 methyl positions in large proteins. The developed methodology has been applied to an 82-kDa enzyme MSG. Complete Alaβ and Ileγ2 ^{1}H–^{13}C methyl chemical shift assignments could be obtained from the developed set of sensitive 3D experiments. Although [U–^{13}C]-labeled pyruvate has been used as the main carbon source in the D_2O-based bacterial medium to generate selectively protonated Alaβ and Ileγ2 positions in [U–^{13}C]-MSG in this work, the described methodology for methyl assignments should be applicable to protein molecules within $\sim$100-kDa molecular weight range *irrespective* of the labeling strategy chosen to produce (selectively) protonated Alaβ and Ileγ2 $^{13}CH_3$ sites on a deuterated background. The obtained assignments represent the first step in an attempt to extend the selective methyl labeling methodology for large proteins beyond commonly used ILV sites.

Acknowledgment This work was supported in part by the Nano-Biotechnology Award to V.T. The authors thank Prof. David Fushman (University of Maryland) for useful discussions.

References

Bax A, Griffey RH, Hawkings BL (1983) Correlation of proton and nitrogen-15 chemical shifts by multiple quantum NMR. J Magn Reson 55:301–315

Boyd J, Soffe N (1989) Selective excitation by pulse shaping combined with phase modulation. J Magn Reson 85:406–413

Delaglio F, Grzesiek S, Vuister GW, Zhu G, Pfeifer J, Bax A (1995) NMRPipe: a multidimensional spectral processing system based on UNIX pipes. J Biomol NMR 6:277–293

Fernandez A, Scott LR, Scheraga HA (2003) Insufficiently dehydrated hydrogen bonds as determinants of protein interactions. J Phys Chem 107:9929–9932

Gardner KH, Kay LE (1998) The use of ^{2}H, ^{13}C, ^{15}N multidimensional NMR to study the structure and dynamics of proteins. Annu Rev Biophys Biomol Struct 27:357–406

Gardner KH, Rosen MK, Kay LE (1997) Global folds of highly deuterated, methyl protonated proteins by multidimensional NMR. Biochemistry 36:1389–1401

Geen H, Freeman R (1991) Band-selective radiofrequency pulses. J Magn Reson 93:93–141

Goto NK, Gardner KH, Mueller GA, Willis RC, Kay LE (1999) A robust and cost-effective method for the production of Val, Leu, Ile (δ1) methyl-protonated 15N-, 13C-, 2H-labeled proteins. J Biomol NMR 13:369–374

Guo C, Tugarinov V (2009) Identification of HN-methyl NOEs in large proteins using simultaneous amide-methyl TROSY-based detection. J Biomol NMR 43:21–30

Hamel DJ, Dahlquist FW (2005) The contact interface of a 120 kD CheA-CheW complex by methyl TROSY interaction spectroscopy. J Am Chem Soc 127:9676–9677

Howard BR, Endrizzi JA, Remington SJ (2000) Crystal structure of *Escherichia coli* malate synthase G complexed with magnesium and glyoxylate at 2.0 A resolution: mechanistic implications. Biochemistry 39:3156–3168

Isaacson RL, Simpson PJ, Liu M, Cota E, Zhang X, Freemont P, Matthews S (2007) A new labeling method for methyl transverse relaxation-optimized spectroscopy NMR spectra of alanine residues. J Am Chem Soc 129:15428–15429

Johnson BA, Blevins RA (1994) NMRView: a computer program for the visualization and analysis of NMR data. J Biomol NMR 4:603–614

Kay LE, Ikura M, Tschudin R, Bax A (1990) Three-dimensional triple-resonance NMR spectroscopy of isotopically enriched proteins. J Magn Reson 89:496–514

Marion D, Ikura M, Tschudin R, Bax A (1989) Rapid recording of 2D NMR spectra without phase cycling. Application to the study of hydrogen exchange in proteins. J Magn Reson 85:393–399

McCaldon P, Argos P (1988) Oligopeptide biases in protein sequences and their use in predicting protein coding regions in nucleotide sequences. Proteins 4:99–122

McCoy MA, Mueller L (1992) Selective shaped pulse decoupling in NMR: homonuclear ^{13}C-carbonyl decoupling. J Am Chem Soc 114:2108–2112

Mueller L (1979) Sensitivity enhanced detection of weak nuclei using heteronuclear multiple quantum coherence. J Am Chem Soc 101:4481–4484

Nuzillard JM, Freeman R (1994) Oversampling in two-dimensional NMR. J Magn Reson A 110:252–258

Ollerenshaw JE, Tugarinov V, Kay LE (2003) Methyl TROSY: explanation and experimental verification. Magn Reson Chem 41:843–852

Patt SL (1992) Single- and multiple-frequency-shifted laminar pulses. J Magn Reson 96:94–102

Rosen MK, Gardner KH, Willis RC, Parris WE, Pawson T, Kay LE (1996) Selective methyl group protonation of perdeuterated proteins. J Mol Biol 263:627–636

Shaka AJ, Keeler J, Frenkiel T, Freeman R (1983) An improved sequence for broadband decoupling: WALTZ-16. J Magn Reson 52:335–338

Shaka AJ, Barker PB, Freeman R (1985) Computer-optimized decoupling scheme for wideband applications and low-level operation. J Magn Reson 64:547–552

Sheppard D, Guo C, Tugarinov V (2009) 4D ^{1}H–^{13}C NMR spectroscopy for assignments of alanine methyls in large and complex protein structures. J Am Chem Soc 131:1364–1365

Sprangers R, Kay LE (2007) Quantitative dynamics and binding studies of the 20S proteasome by NMR. Nature 445:618–622

Sprangers R, Velyvis A, Kay LE (2007) Solution NMR of supramolecular complexes: providing new insights into function. Nat Methods 4:697–703

Tugarinov V, Kay LE (2003) Ile, Leu, and Val methyl assignments of the 723-residue malate synthase G using a new labeling strategy and novel NMR methods. J Am Chem Soc 125:13868–13878

Tugarinov V, Kay LE (2004) An isotope labeling strategy for methyl TROSY spectroscopy. J Biomol NMR 28:165–172

Tugarinov V, Muhandiram R, Ayed A, Kay LE (2002) Four-dimensional NMR spectroscopy of a 723-residue protein: chemical shift assignments and secondary structure of malate synthase G. J Am Chem Soc 124:10025–10035

Tugarinov V, Hwang PM, Ollerenshaw JE, Kay LE (2003) Cross-correlated relaxation enhanced ^{1}H–^{13}C NMR spectroscopy of methyl groups in very high molecular weight proteins and protein complexes. J Am Chem Soc 125:10420–10428

Tugarinov V, Hwang PM, Kay LE (2004) Nuclear magnetic resonance spectroscopy of high-molecular-weight proteins. Annu Rev Biochem 73:107–146

Velyvis A, Yang YR, Schachman HK, Kay LE (2007) A solution NMR study showing that active site ligands and nucleotides directly perturb the allosteric equilibrium in aspartate transcarbamoylase. Proc Natl Acad Sci USA 104:8815–8820

Venters RA, Farmer BT, Fierke CA, Spicer LD (1996) Characterizing the use of perdeuteration in NMR Studies of large proteins: ^{13}C, ^{15}N and ^{1}H assignments of human carbonic anhydrase II. J Mol Biol 264:1101–1116

Xu Y, Lin Z, Ho C, Yang D (2005) A general strategy for the assignment of aliphatic side-chain resonances of uniformly ^{13}C, ^{15}N-labeled large proteins. J Am Chem Soc 127:11920–11921

Xu Y, Zheng Y, Fan J-S, Yang D (2006) A new strategy for structure determination of large proteins in solution without deuteration. Nat Methods 3:931–937